Virologica Sinica 41 (2026) 651–661

Contents lists available at ScienceDirect

Virologica Sinica

journal homepage: www.keaipublishing.com/en/journals/virologica-sinica
www.virosin.org

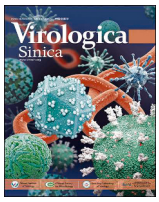

Research Article

EV-A71 induces GSDME-dependent T-cell pyroptosis: A novel mechanism and MeCbl therapeutic potential

Chong Wang [a], Bingyu Guo [a], Yilin Li [a,b], Xi Zhou [a,b], Zongqiang Cui [a,b,*], Yujie Ren [a,b,*]

[a] State Key Laboratory of Virology and Biosafety, Wuhan Institute of Virology, Center for Biosafety Mega-Science, Chinese Academy of Sciences, Wuhan 430071, China
[b] University of Chinese Academy of Sciences, Beijing 100049, China

ARTICLE INFO

Keywords:
Enterovirus A71 (EV-A71)
T cells
Immune responses
GSDME-Dependent pyroptosis
Methylcobalamin

ABSTRACT

Enterovirus A71 (EV-A71) is the primary pathogen causing severe hand-foot-and-mouth disease (HFMD) in young children, with T-cell immune dysfunction closely linked to severe clinical outcomes. However, the molecular mechanisms underlying EV-A71-mediated T-cell impairment remain unclear, and no specific therapies are currently available. Here, we investigated the interaction between EV-A71 and T cells, and explored potential targeted therapeutic strategies. Our results showed that EV-A71 efficiently infects T cell lines (Jurkat, EL-4) and primary mouse $CD3^+$ T cells in a dose- and time-dependent manner, inducing T-cell death and upregulating pro-inflammatory cytokines (IL-1β, IL-6, TNF-α). Mechanistically, EV-A71 infection triggers GSDME-dependent pyroptosis in T cells via caspase-3 activation, rather than GSDMD-dependent pyroptosis, as evidenced by genetic ablation and inhibitor experiments. Methylcobalamin (MeCbl), a specific GSDME inhibitor, rescued EV-A71-induced T-cell loss, and significantly improved the survival rate (80%) of EV-A71-infected newborn mice. Furthermore, the combined treatment with MeCbl and AGS-A (a T cell-dependent therapeutic agent) exerted a synergistic protective effect, achieving 90% survival rate in wild-type mice, which was abrogated in T cell-deficient BALB/c-$nu^{-/-}$ mice. Collectively, our findings identify GSDME-dependent T-cell pyroptosis as a key pathogenic mechanism of EV-A71 infection and highlight MeCbl as a promising targeted agent for HFMD treatment, either used alone or in combination with AGS-A.

INTRODUCTION

Enteroviruses are a large group of non-enveloped, positive-sense and single-stranded RNA viruses belonging to the genus *Enterovirus* of the family *Picornaviridae*. This genus encompasses numerous critical human pathogens, including poliovirus, enterovirus A71 (EV-A71), coxsackieviruses, and echoviruses, which collectively cause approximately 3 billion human infections annually worldwide. Clinical manifestations of enteroviral infections range from mild conditions such as upper respiratory tract illness and common cold to severe, life-threatening outcomes, including severe hand-foot-and-mouth disease (HFMD), aseptic meningitis, encephalitis, myocarditis, neonatal sepsis-like disease, and poliomyelitis.

HFMD is a prevalent pediatric infectious disease primarily caused by EV-A71 and other enteroviruses such as coxsackievirus A16 (CV-A16) and A6 (CV-A6) (Chan et al., 2000; Fioravanti, 2012; Ho et al., 1999; Tan et al., 2011). Each year, millions of HFMD cases occur in children under 5 years of age globally, with high contagiousness facilitating rapid spread in schools and kindergartens. Among HFMD-causing pathogens, the neurotropic EV-A71 is the leading cause of severe central nervous system (CNS) complications and accounts for the majority of HFMD-related fatalities (Huang et al., 1999; Solomon et al., 2010).

* Corresponding authors.
E-mail addresses: renyujie@wh.iov.cn (Y. Ren), czq@wh.iov.cn (Z. Cui).
Peer review under the responsibility of editorial board of *Virologica Sinica*.

https://doi.org/10.1016/j.virs.2026.05.006
Received 3 February 2026; Accepted 22 May 2026
Available online 29 May 2026

Consequently, EV-A71 is recognized as the most virulent HFMD-associated enterovirus and poses a significant threat to global child health. Notably, no specific antiviral drugs or effective therapies are currently available for the treatment of EV-A71 infection or HFMD.

Although EV-A71 infection and HFMD can occur in both children and adults, adult infection of this virus is usually asymptomatic, while severe symptoms are predominantly occur in children at preschool ages. Compared with adults, young children have immature cellular immunity, which is pivotal for viral control (Carsetti et al., 2020; Olin et al., 2018; Simon et al., 2015). Besides, a number of clinical observations have indicated the correlation between compromised cellular immunity and severe symptoms of EV-A71 infection (Chang et al., 2006, 2008; Yang et al., 2001). Moreover, our published research has demonstrated that EV-A71 infection dramatically impairs T-cell immune response, and the dysfunction of T-cell immunity contributes to the pathogenesis of EV-A71 infection (Wang et al., 2025). However, the specific molecular mechanisms by which EV-A71 infection disrupts T-cell immune responses remain unclear, which hinders the development of effective therapeutic strategies for HFMD.

Pyroptosis, an inflammatory form of programmed cell death, is tightly regulated by gasdermin (GSDM) family proteins, with GSDMD and GSDME being key mediators of distinct pyroptotic pathways (He et al., 2015; Shi et al., 2015; Zhang et al., 2021). Given the critical role of T cells in anti-EV-A71 immunity and the link between T-cell dysfunction and severe infection, we hypothesized that EV-A71 may target T cells directly to disrupt immune function, potentially via inducing pyroptosis. Herein, we report that EV-A71 efficiently infects T cells, induces GSDME-dependent pyroptosis, and triggers pro-inflammatory responses. Furthermore, we demonstrate that methylcobalamin (MeCbl), a specific GSDME inhibitor, rescues EV-A71 impaired T-cell immune function and exerts potent *in vivo* therapeutic effects against EV-A71 infection. Importantly, the synergistic protective effect of MeCbl combined with AGS-A (a previously identified T cell-dependent therapeutic agent) is dependent on intact T-cell populations, highlighting the critical role of T-cell protection in effective therapeutic strategies against EV-A71 infection.

RESULTS

EV-A71 efficiently infects T cells, induce their death, and trigger the activation of inflammation

To determine whether EV-A71 directly infects T lymphocytes, Jurkat, EL-4 cells were used to infect with EV-A71 at the different multiplicity of infections (MOI) of 0.5, 1.0 and 5.0, and the replicative efficiencies of EV-A71 in different cells were determined via examining the viral RNA accumulation at 24 hours post infection (h.p.i.) with qRT-PCR. Our data showed that the T cell lines, including Jurkat and EL-4, can support EV-A71 infection (Fig. 1A, C). We also examined viral RNA levels at 12, 24, and 36 h.p.i. with a multiplicity of infection (MOI) of 1 (Fig. 1B, D). The results indicate that EV-A71 is not only capable of infecting T-cell lines but can also replicate effectively within them. Besides, EV-A71 infection induced Jurkat and EL-4 cells death, which was examined by the release of the cytosolic enzyme lactate dehydrogenase (LDH) (Fig. 1E, I). Moreover, we found that the mRNA levels of pro-inflammatory genes, including *IL-1β*, *IL-6* and *TNF-α*, were significantly stimulated in EV-A71-infected Jurkat (Fig. 1F–H) and EL-4 cells (Fig. 1J–L). We further examined the EV-A71 infection and replication in CD3 T cells from C57BL/6 mice, similar to the data from T cell lines, our data showed that EV-A71 infected CD3 T cell in a dose- and time-dependent manner (Fig. 1M and N). The LDH was determined in cellular supernatants (Fig. 1O) and pro-inflammatory genes (Fig. 1P–R) were also found to be upregulated in EV-A71-infected CD3 T cell. Together, our findings indicate that EV-A71 can efficiently infect T cells, induce cell death and trigger the activation of inflammation.

EV-A71 infection induces T cell pyroptotic death depending on GSDME

Pyroptosis is a typical form of inflammatory cell death (Shi et al., 2015; Zhang et al., 2021) The observations showed that EV-A71 infection induced T cell death accompanied by inflammatory activation, gave us a hint that EV-A71 infection may induce pyroptosis in T cells. To validate this possibility, we examined the cleavage of caspase 1 as well as the cleavage of GSDMD, and the cleavage of caspase 3 as well as the cleavage of GSDME, the hallmarks of pyroptosis (Shi et al., 2015; Zhang et al., 2021), in Jurkat cells infected with 1 MOI EV-A71 at 12, 24 and 36 h.p.i. Jurkat cells treated with lipopolysaccharides (LPS) plus Nigericin (GSDMD-dependent pyroptosis) or Doxorubicin (DOX, GSDME-dependent pyroptosis) were used as the positive control. Western blotting analyses uncovered that EV-A71 infection does not induce cleavage of caspase 1 or GSDMD (Fig. 2A), nor is cleavage of GSDME observed (Fig. 2B). However, it can trigger cleavage of caspase-3 (Fig. 2B). Further analysis of the data revealed that GSDME expression is minimal in Jurkat cells (Fig. 2B), which aligns with previously reported data (Wang Y.P. et al., 2017). When EV-A71 infected Jurkat cells overexpressing GSDME, cleavage of GSDME was observed after EV-A71 infection (Fig. 2C). Therefore, these findings indicate that EV-A71 infection induces GSDME-dependent pyroptosis in Jurkat cells.

We further examined the EV-A71-induced pyroptosis in CD3 T cells from C57BL/6 mice. Similar to the data from Jurkat cells, the data showed that EV-A71 infection does not induce cleavage of caspase 1 or GSDMD (Fig. 2D), but the cleavage of GSDME and caspase-3 were observed (Fig. 2E). Moreover, we constructed Jurkat cell lines stably expressing ShRNAs targeting the gene of GSDMD and GSDME, respectively (Fig. 3A, D). The viral RNA replication of EV-A71 was not affected by knocking down GSDMD or GSDME (Fig. 3B, E). Our data showed that EV-A71 infection or LPS plus Nigericin treatment induced cell death in Jurkat cells, which was examined by the release of the LDH, and these activations were remarkably attenuated by knocking down GSDME, but not by knocking down GSDMD (Fig. 3C, F). Besides, Z-DEVD-FMK (caspase-3 inhibitor) treatment abrogated the cleavage of caspase-3 and GSDME in Jurkat and CD3 T cells infected with EV-A71 (Fig. 3G and H). Together, our findings uncover that EV-A71 induces GSDME-dependent pyroptotic cell death in T cells.

Methylcobalamin (MeCbl) treatment protected from lethal EV-A71 infection in mice

We further assessed the physiological relevance of EV-A71-induced T cell pyroptosis *in vivo*. MeCbl has been reported as a specific inhibitor of GSDME, capable of significantly suppressing GSDME-dependent pyroptosis (Xu et al., 2025). We sought to determine whether the action of MeCbl to treat EV-A71 infection in mice is associated with the immune response of T cells. We treated 5-day-old ICR mice with MeCbl via intraperitoneal (i.p.) administration at a dose of 10 mg/kg 24 h after EV-A71 challenge, followed by treatment once every other day for three times (Fig. 4A). Our data showed that MeCbl treatment did not enhance the percentages of $CD3^+$ total T cells in spleens of non-infected 5-day-old ICR mice, but it effectively restored the proportion of T cells to the same level as that in mice not infected with EV-A71 (Fig. 4B and C).

We further assess the therapeutic potential of MeCbl on EV-A71 infection. The mice were treated with the same method shown in Fig. 4A. The results showed that the mice in the vehicle group (control) began to succumb to EV-A71 infection from 8 d.p.i., and reached 60% mortality at 11 d.p.i. In contrast, 80% of the mice in the MeCbl therapeutic group survived the viral challenge (Fig. 4D). Consistently, we observed significant differences of body weights and clinical scores between the therapeutic and control groups (Fig. 4E and F). In addition, the viral RNA accumulations of EV-A71 in muscle, spleen, and brain tissues were significantly reduced in the MeCbl therapeutic group compared with those in the control group at both 5 and 7 d.p.i. (Fig. 4G).

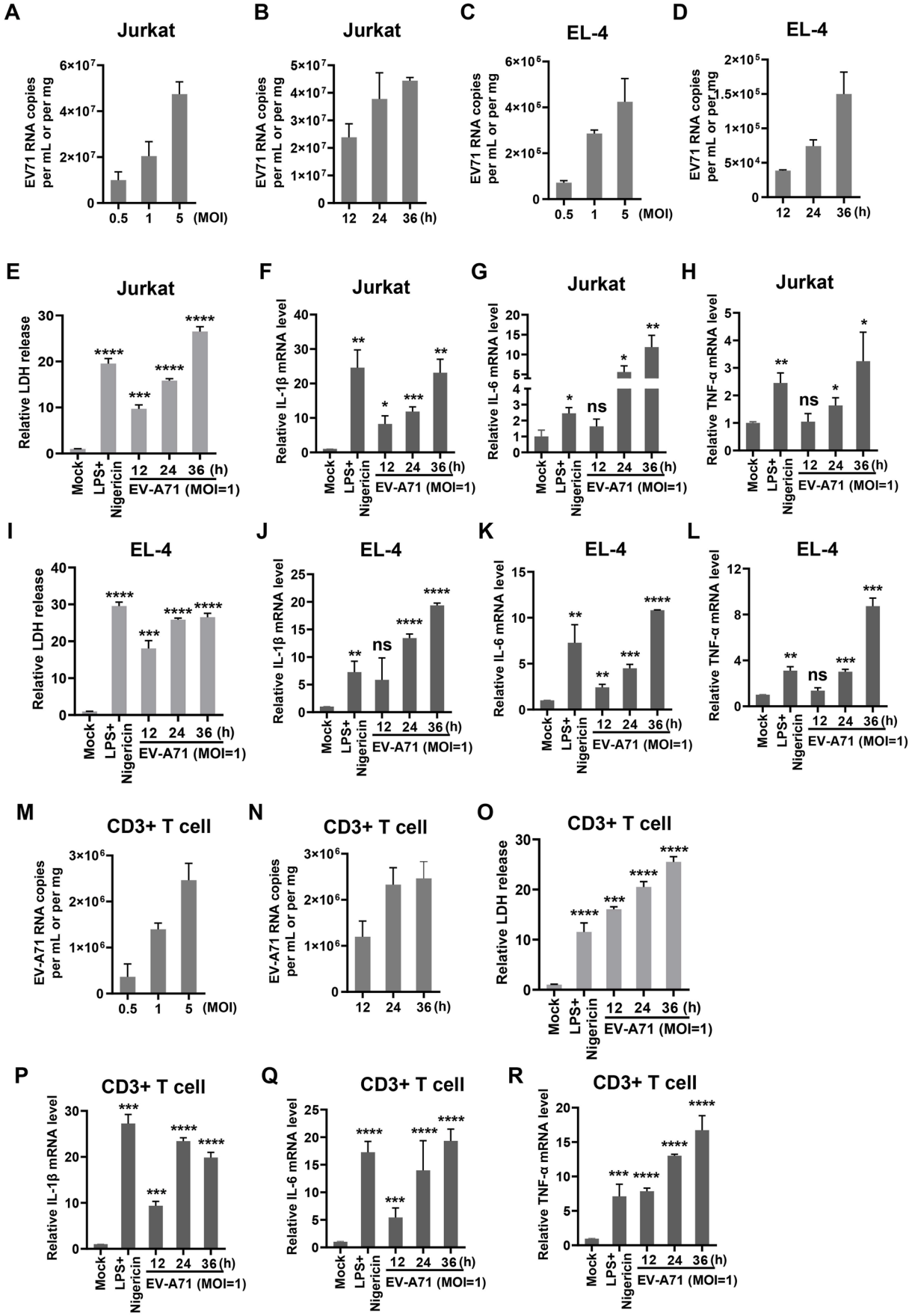

(caption on next page)

Fig. 1. EV-A71 efficiently infects T cells, induce their death, and trigger the activation of inflammation. Jurkat (**A**) or EL-4 (**C**) cells were infected with EV-A71 at an MOI of 0.5, 1 or 5 for 24 h or Jurkat (**B, E–H**) or EL-4 (**D, I–L**) or mouse $CD3^+$ T (**M–R**) cells were infected with EV-A71 at an MOI of 1 for 12, 24 or 36 h. Cells treated with lipopolysaccharides (LPS, 10 μg/mL) for 5 h and 10 μM Nigericin for 1 h was used as the positive control, while cells without treatment (Mock) were used as the negative control. Total RNAs were extracted and the accumulation of viral RNA was measured via qRT-PCR, and the level of viral RNA in uninfected cells (mock) was defined as 1-fold (**A–D, M–N**). The lactate dehydrogenase (LDH) release in the supernatants were determined by cytotoxicity assay, and the level of LDH in mock cells was defined as 1-fold (**E, I, O**). The intracellular mRNA levels of IL-1β (**F, J, P**), IL-6 (**G, K, Q**) and TNF-α (**H, L, R**) were measured by qRT-PCR, and the level of IL-1β, IL-6 and TNF-α mRNA in mock cells were defined as 1-fold. Data are representative of three independent experiments. Graph shows mean ± SEM. *P* values were calculated via ANOVA. *, $P < 0.05$; **, $P < 0.01$; ***, $P < 0.001$; ****, $P < 0.0001$; ns, not significant.

Moreover, MeCbl treatment failed to inhibit EV-A71 replication in Jurkat cells (Supplementary Fig. S1A), ruling out the possibility that MeCbl directly targets the life cycle of EV-A71. In addition, MeCbl showed minimal cytotoxicity (Supplementary Fig. S1B), further supporting the safety of MeCbl treatment. These results indicate that in the context of viral infection, MeCbl treatment can not only restore the immune response of T cells, but also has potent *in vivo* therapeutic efficacy against EV-A71 infection in newborn mice.

The combination of MeCbl and AGS-A treatment exerts a synergistic protective effect in mice infected with EV-A71 depending on T cells

The therapeutic effect of AGS-A is dependent on the presence of T cells in our previous study (Wang et al., 2025). We next assessed whether the combination of MeCbl and AGS-A treatment exerts a synergistic protective effect in mice infected with EV-A71. We treated 5-day-old WT BALB/c mice with MeCbl via i.p. administration at a dose of 10 mg/kg 24 h after EV-A71 challenge, followed by treatment once every two days for three times, and administrated AGS-A via i.p. at a dose of 10 mg/kg 12 h after EV-A71 challenge, followed by treatment twice a day for 6 days. The mice began to succumb to EV-A71 infection from 6 d.p.i., and reached 80% mortality at 11 d.p.i. In contrast, 60% of the mice in the MeCbl therapeutic group survived the viral challenge, and 90% of the mice in the combination of MeCbl and AGS-A therapeutic group survived the viral challenge (Fig. 5A and B). Consistently, we observed significant differences of body weights and clinical scores between the therapeutic and control groups (Fig. 5C and D). The data show that combination of MeCbl and AGS-A treatment exerts a synergistic protective effect in mice infected with EV-A71.

We further assessed whether the synergistic protective effect is dependent on the presence of T cells. We took advantage of BALB/c-nu$^{-/-}$ mice that lack T cells, and examined the effects of combination with MeCbl and AGS-A treatment on BALB/c-nu$^{-/-}$ mice challenged with EV-A71. The results showed that this saponin compound failed to show any synergistic protective effect in the aspects of survival rate, body weights, and clinical scores, on the lethal EV-A71 challenge when being compared with non-treated, EV-A71-infected group in the 10-day-old BALB/c-nu$^{-/-}$ mice (Fig. 5E–G). These results show that the therapeutic effect of combination with MeCbl and AGS-A is dependent on T cells.

DISCUSSION

Enterovirus A71 (EV-A71) remains a major threat to pediatric health worldwide, with severe cases closely linked to compromised cellular immunity. Previous studies have established that EV-A71 impairs T cell function, but the underlying molecular mechanisms have long been elusive. In this study, we demonstrate for the first time that EV-A71 efficiently infects T cells and induces GSDME-dependent pyroptosis, which contributes to T cell loss and immune dysfunction. Furthermore, targeted inhibition of GSDME by MeCbl rescues T cell immunity and exerts potent therapeutic effects against EV-A71 infection, alone or in combination with AGS-A. These findings provide novel insights into EV-A71 pathogenesis and identify GSDME as a promising therapeutic target for HFMD.

T cells are central to antiviral defense, and their dysfunction is a hallmark of severe EV-A71 infection (Shen et al., 2019; Wei et al., 2012; Zhao et al., 2020). While EV-A71 was traditionally considered to primarily target epithelial and neural cells, our data clearly show that T cell lines (Jurkat, EL-4) and primary mouse $CD3^+$ T cells support efficient EV-A71 infection and replication in a dose- and time-dependent manner (Fig. 1A–D). This direct infection of T cells is a critical observation, as it suggests EV-A71 can directly subvert the adaptive immune response rather than merely exploiting pre-existing immune deficiencies in young children. Consistent with this, EV-A71-infected T cells exhibit robust upregulation of pro-inflammatory cytokines (IL-1β, IL-6, TNF-α) (Fig. 1F–H, J–L, M–O), which may contribute to the systemic inflammation observed in severe HFMD. These results align with clinical reports of elevated pro-inflammatory cytokines in EV-A71-infected patients with neurological complications (Lee, 2016), highlighting the pathological relevance of T cell-derived inflammation.

Pyroptosis is an inflammatory form of programmed cell death mediated by gasdermin (GSDM) family proteins, with GSDMD and GSDME being the most well-characterized (De Schutter et al., 2021; Liu et al., 2016; Xu et al., 2018). GSDMD is typically activated by caspase-1 downstream of inflammasomes, while GSDME is cleaved by caspase-3 to trigger pyroptosis (Broz et al., 2020; Rogers et al., 2019; Wu et al., 2018). Our study reveals a unique pyroptotic pathway in EV-A71-infected T cells: EV-A71 induces caspase-3 activation and subsequent cleavage of GSDME, but not caspase-1 or GSDMD (Fig. 2A and B). This finding is particularly significant given the emerging role of GSDME in immune cell death. While GSDMD-dependent pyroptosis is well-documented in macrophages and neutrophils, GSDME-dependent pyroptosis has been primarily reported in cancer cells and epithelial cells (Wang Y.P. et al., 2017; Wu et al., 2018). Our study extends this to T cells, identifying GSDME as a key mediator of EV-A71-induced T cell death. Notably, T cell pyroptosis differs from apoptosis in its pro-inflammatory nature: the release of cytoplasmic contents during pyroptosis amplifies inflammation, which may exacerbate tissue damage in EV-A71-infected individuals. This dual effect T cell loss and inflammation amplification provides a mechanistic explanation for the link between compromised cellular immunity and severe HFMD.

The identification of GSDME-dependent pyroptosis as a driver of T cell loss prompted us to evaluate the therapeutic potential of GSDME inhibition. MeCbl, a specific GSDME inhibitor (Xu et al., 2025), effectively rescued EV-A71-induced T cell depletion *in vivo*, restoring T cell proportions to uninfected levels. Importantly, MeCbl treatment significantly improved survival, reduced viral loads in key tissues (muscle, spleen, brain), and alleviated clinical symptoms in EV-A71-infected newborn mice. This therapeutic efficacy is likely mediated by preserving T cell function, as T cells are critical for controlling viral replication (Simon et al., 2015). Notably, MeCbl did not directly inhibit viral replication in T cells (Supplementary Fig. S1), emphasizing that its protective effect is immune-mediated. This is a key distinction from conventional antiviral drugs, which target viral enzymes or entry (Lu et al., 2021); the immunomodulatory role of MeCbl could be highly dependent and relies on a fully functional immune system, which explains the phenotypic discrepancy between in vitro GSDME knockdown and *in vivo* MeCbl treatment. In vitro isolated cells lack the integrated immune network and cell-cell crosstalk required for immune mediated antiviral effects, so GSDME silencing alone fails to alter viral RNA accumulation; in contrast, in intact immunocompetent mice, MeCbl rescues immune cell function, suppresses detrimental pyroptosis, and enhances host antiviral resistance collectively.

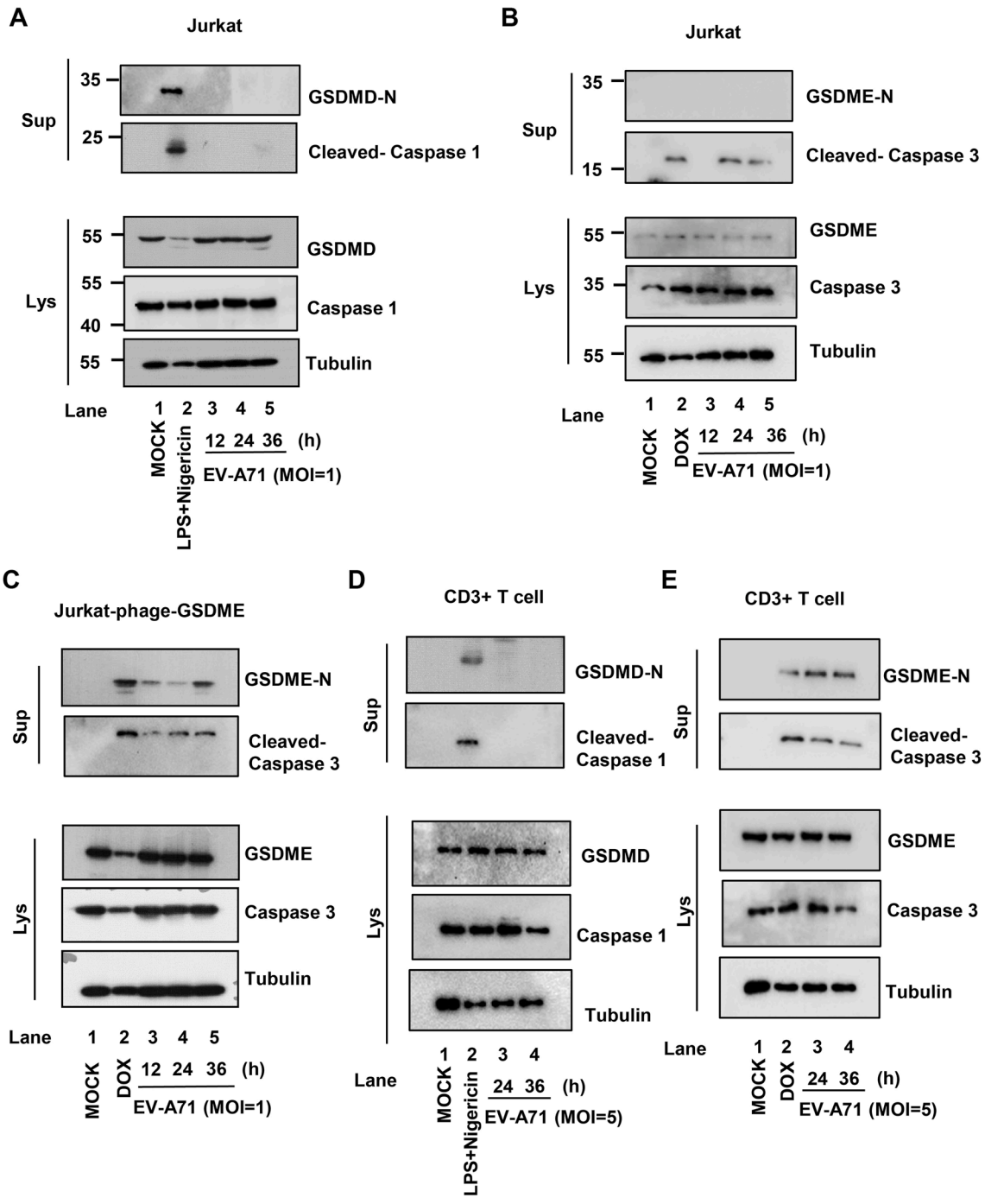

Fig. 2. EV-A71 infection induces T cell pyroptotic death depending on GSDME. Jurkat (**A, B**), Jurkat-phage-GSDME (**C**) and $CD3^+$ T cells (**D, E**) were infected with EV-A71 at an MOI of 1 for 12, 24 or 36 h. Cells treated with lipopolysaccharides (LPS, 10 μg/mL) for 5 h and 10 μM Nigericin for 1 h was used as the positive control (GSDMD-dependent pyroptosis) or cells treated with Doxorubicin (DOX) (1 μM) for 6–12 h were used as the positive control (GSDME-dependent pyroptosis), while cells without treatment (Mock) were used as the negative control. GSDMD-N and cleaved-caspase 1 in the supernatants (Sup), and GSDMD and caspase 1 in cell lysates (Lys) were examined by Western blotting with the indicated antibodies. Cleavage of caspase-1 and GSDMD in the supernatants, and GSDMD or caspase-1 in the lysates were examined by Western blotting (**A, D**). Cleavage of caspase-3 and GSDME in the supernatants, and GSDME or caspase-3 in the lysates were examined by Western blotting (**B, C, E**).

Furthermore, the synergistic protective effect of MeCbl and AGS-A (a previously identified anti-EV-A71 compound) underscores the importance of T cells in therapeutic efficacy. The combination of MeCbl (which preserves T cells) and AGS-A (which may enhance T cell-dependent antiviral immunity) achieved 90% survival in WT mice, compared to 60% with MeCbl alone and 80% mortality in controls. Critically, this synergistic effect was absent in T cell-deficient BALB/c-nu$^{-/-}$ mice, confirming that T cells are required for the combined therapy to work. Moreover, T cells serve as a pivotal cellular hub mediating the protective efficacy of MeCbl, as verified by our T cell-deficient mouse model. In WT immunocompetent mice, EV-A71 infection elicits aberrant GSDME-dependent pyroptosis in T lymphocytes, which are critical for antiviral adaptive immunity; this massive pyroptotic cell death triggers acute T cell depletion, cripples the host's ability to clear the virus, and exacerbates systemic inflammation and tissue injury. MeCbl effectively blocks GSDME pore formation and subsequent

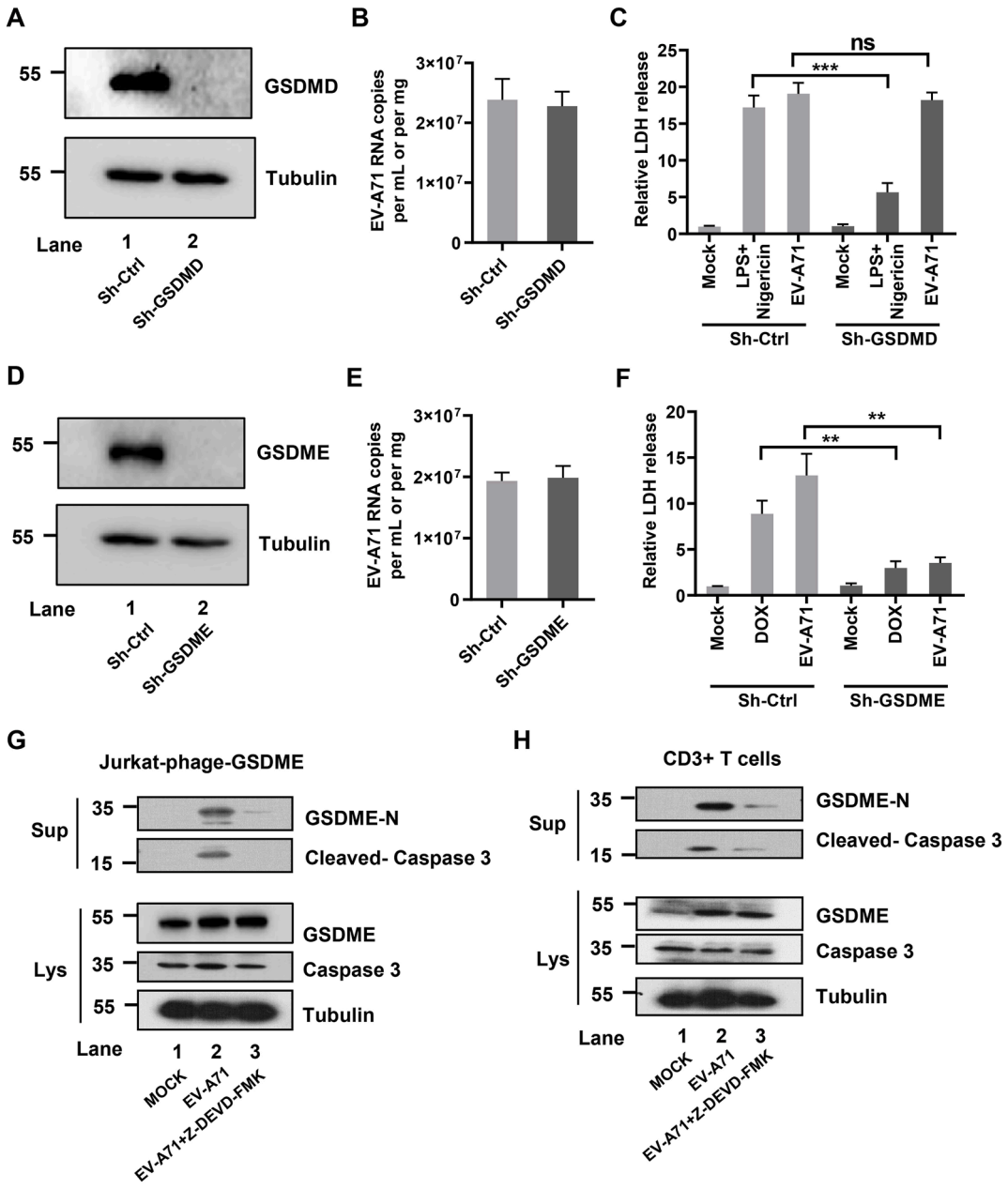

Fig. 3. Caspase 3 and GSDME are essential for EV-A71-induced pyroptosis. **A–C** Jurkat cells stably expressing control shRNA (Ctrl) or specific shRNA targeting GSDMD were treated with lipopolysaccharides (LPS) plus Nigericin or infected with EV-A71 at an MOI of 1 for 24 h. **D–F** Jurkat cells stably expressing control shRNA (Ctrl) or specific shRNA targeting GSDME were treated with DOX or infected with EV-A71 at an MOI of 1 for 24 h. GSDMD and GSDME in the lysates were examined by Western blotting (**A, D**). Total RNAs were extracted and the accumulation of viral RNA was measured via qRT-PCR, and the level of viral RNA in uninfected cells (mock) was defined as 1-fold (**B, E**). The LDH release in the supernatants were determined by cytotoxicity assay, and the level of LDH in mock cells was defined as 1-fold (**C, F**). Data are representative of three independent experiments. Graph shows mean ± SEM. *P* values were calculated via ANOVA. ; **, $P < 0.01$; ***, $P < 0.001$; ns, not significant. Jurkat-phage-GSDME and $CD3^+$ T cells were infected with EV-A71 at an MOI of 1 for 24 h, and cells treated with caspase-3 inhibitor Z-DEVD-FMK (50 μM) were used as the control. GSDME-N or cleavage of caspase-3 in the supernatants, and GSDME or caspase-3 in the lysates were examined by Western blotting (**G, H**).

pyroptotic signaling in T cells, could preserving the quantity and functional integrity of T cells, and reinstating the host's adaptive immune surveillance to eliminate infected cells and restrict viral proliferation. Of note, the detailed and specific immunoregulatory mechanism will be further investigated in the future study.

Our findings have several important implications for EV-A71 research and clinical practice. First, they provide a novel mechanistic framework for EV-A71-induced immune dysfunction, identifying GSDME-dependent T cell pyroptosis as a key pathogenic event. This advances our understanding of why young children with less developed T cell immunity are more susceptible to severe EV-A71 infection (Carsetti et al., 2020): their T cells may be more prone to pyroptosis, leading to exacerbated immune loss. Second, GSDME emerges as a promising therapeutic target for HFMD, with MeCbl representing a lead compound for further development. Given the lack of specific antivirals for EV-A71, targeted inhibition of GSDME could fill a critical unmet medical need. Third, the synergistic effect of MeCbl and AGS-A suggests that combining immune-modulating agents with direct antivirals may be a viable strategy for treating severe EV-A71 infections.

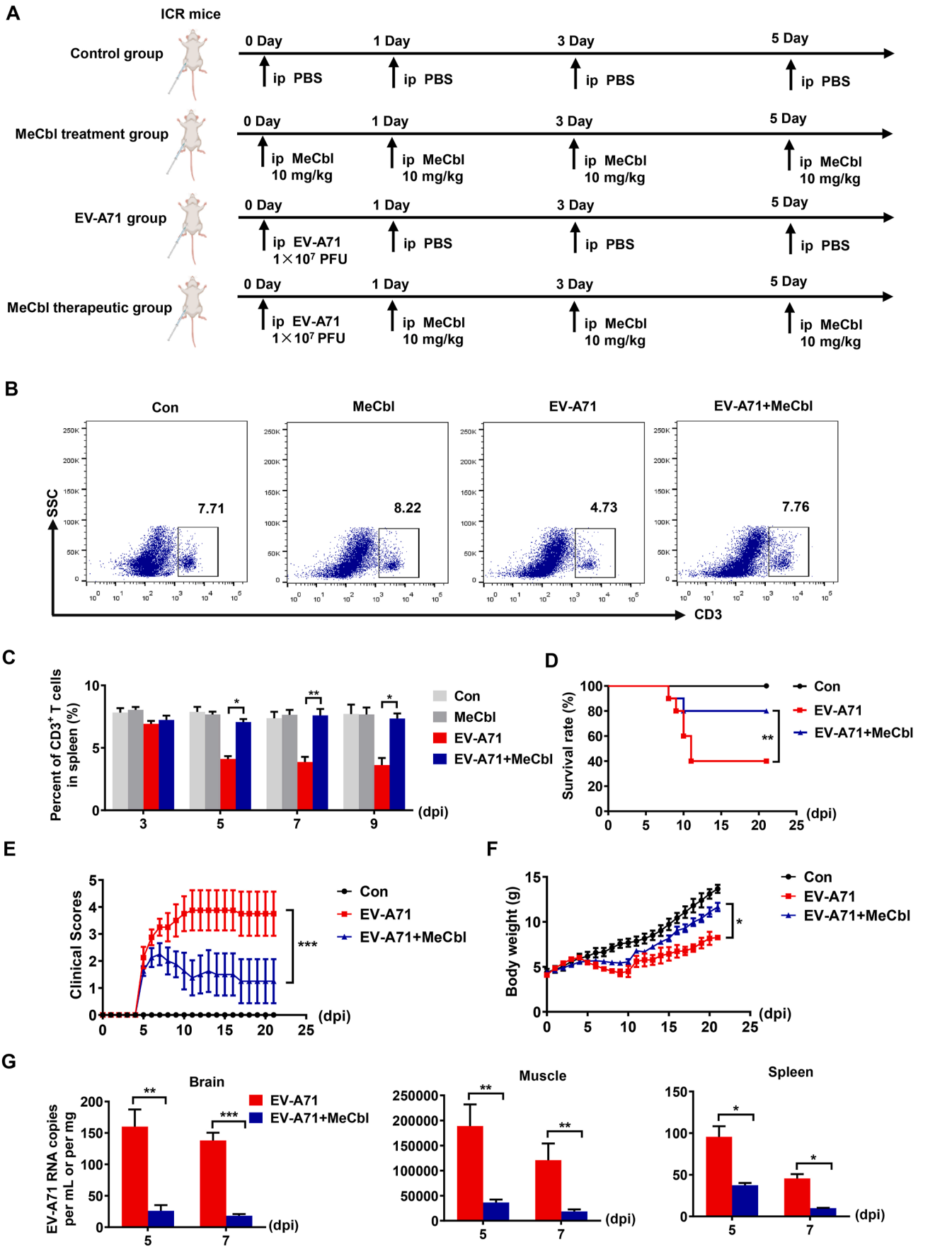

(caption on next page)

Fig. 4. Methylcobalamin (MeCbl) treatment protected from lethal EV-A71 infection in mice. **A** 5-day-old ICR mice were treated with MeCbl (10 mg/kg) or PBS via intraperitoneal (i.p.) administration 24 h after EV-A71 challenge, and control group were treated with PBS, followed by treatment once every other day for three times. **B, C** The percentages of $CD3^+$ T in the spleens of 5-day-old ICR mice in the indicated groups were determined by flow cytometry ($n = 3$ for each group). **D** The survival rates for mice in different groups during the 14-day period are shown by curves. ($n = 10$ for each group). **E, F** Body weights and clinical scores for the mice in (**C**) are plotted. **G** The total cellular RNAs of spleen, muscle and brain tissues collected from EV-A71 infection and MeCbl therapeutic groups were extracted. The viral RNA accumulations in spleen, muscle and brain of ICR mice at 5, 7 dpi were determined via qRT-PCR (**G**). Data are representative of three independent experiments. Graph shows mean ± SEM ($n = 3$). *P* values were calculated via ANOVA. $^*P < 0.05$, $^{**}P < 0.05$, and $^{***}P < 0.001$.

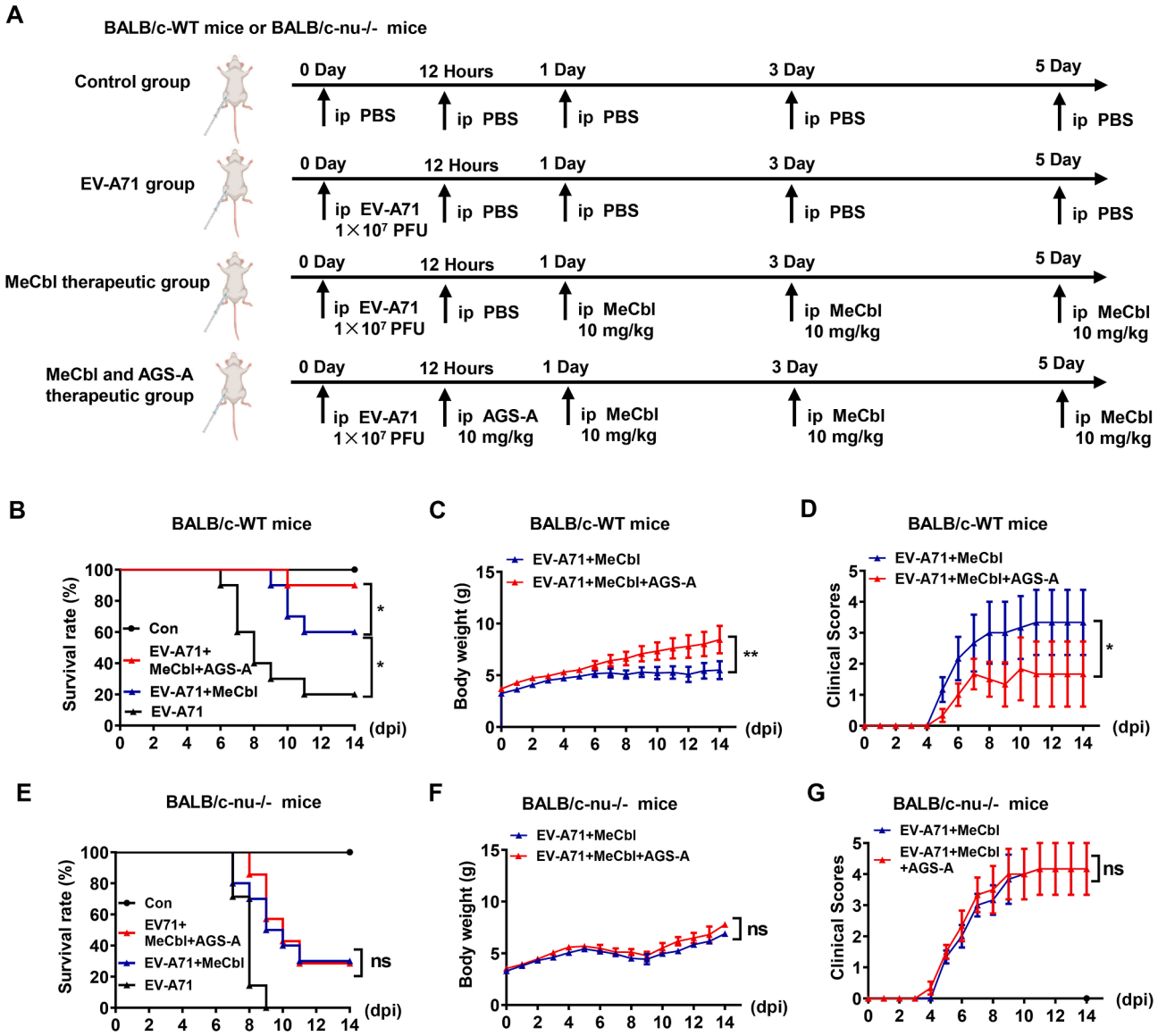

Fig. 5. The combination of MeCbl and AGS-A treatment exerts a synergistic protective effect in mice infected with EV-A71 depending on T cells. **A–G** 5-day-old WT BABL/c (**B–D**) and BALB/c-$nu^{-/-}$ (**E–G**) mice were treated with 10 mg/kg AGS-A 12 h after EV-A71 challenge, and were treated with 10 mg/kg MeCbl 24 h after EV-A71 challenge, followed by AGS-A treatment twice a day for 6 days and MeCbl treatment once every other day for three times. The survival rates of mice in the indicated groups during the 14-day period shown by curves. Body weights and clinical scores for the mice in (**B**) and (**E**) are plotted in (**C, F**) and (**D, G**), respectively. Data are representative of three independent experiments. Graph shows mean ± SEM ($n = 10$). *P* values were calculated via ANOVA. $^*P < 0.05$ and $^{**}P < 0.01$; ns, not significant.

CONCLUSIONS

In conclusion, our study demonstrates that EV-A71 infects T cells and induces GSDME-dependent pyroptosis, leading to T cell loss and immune dysfunction. Targeted inhibition of GSDME with MeCbl rescues T cell immunity and exerts potent therapeutic effects, alone or in combination with AGS-A. These findings not only deepen our understanding of EV-A71 pathogenesis but also provide a novel therapeutic strategy for HFMD.

MATERIAL AND METHODS

Virus

EV-A71 strain H (VR-1432) were obtained from ATCC, the virus was amplified and titers were determined in human rhabdomyosarcoma cells (RD cells) as previously described (Xi et al., 2019). The virus was concentrated by ultrafiltration using Amicon Ultra-15 filters (Millipore, Massachusetts, United States) and quantified by plaque assay.

Experiments including viral infections were conducted in Biosafety Level 2 (BSL-2) labs at Wuhan Institute of Virology.

Cell lines and cultures

Jurkat, EL-4 and RD cell lines were commercially obtained from ATCC. Jurkat and EL-4 cells were cultured in RPMI 1640 medium (Gibco, Massachusetts, United States) supplemented with 10% FBS, 100 U/mL penicillin, and 100 μg/mL streptomycin sulfate. Cells were maintained in an incubator at 37 °C with 5% CO_2. RD cell line was commercially obtained from ATCC and maintained in Dulbecco's modified Eagle's medium (DMEM, Gibco) supplemented with 10% fetal bovine serum (Gibco), 100 U/mL penicillin and 100 μg/mL streptomycin at 37 °C in a humidified atmosphere with 5% CO_2. Mouse CD3 T cells were purified from the spleen of uninfected mice using MoFlo XDP (Beckman Coulter, California, United States). The CD3 T cell were cultured in RPMI 1640 medium (Gibco) supplemented with 10% FBS, 100 U/mL penicillin, and 100 μg/mL streptomycin sulfate in an incubator at 37 °C with 5% CO_2 as our previously reported (Wang C. et al., 2017).

Mice

Pathogen-free 18-day pregnant Institute of Cancer Research (ICR) mice, BALB/c mice, BALB/c-$^{nu-/-}$ mice were obtained from the animal housing facility of the Chinese Academy of Sciences (Changsha, China). All experiments were performed according to protocols approved by the Institutional Animal Care and Use Committee of Wuhan Institute of Virology.

Mice were i.p. injected with 10^7 PFU of EV-A71 in 50 μL of DMEM. Control animals received the same volume of DMEM via the same route. The time before infection was referred to as day 0. Infection with EV-A71 continued for day 10 to day 20 day, and mice presented clinical symptoms at 5 d.p.i. EV-A71-infected mice were sacrificed every other day up to day 9. A score was used to evaluate the clinical symptoms as previously described: 0, healthy; 1, hunchbacked and slow movement; 2, weakness in one limb; 3, paralysis in one limb; 4, paralysis in both limbs; and 5, death (He et al., 2018; Zhang et al., 2013). The spleen, brain and muscle of each mouse was collected and total RNAs from spleen were extracted with TRIzol (10296010) (Invitrogen, California, United States). The viral RNA accumulation was determined via RT-qPCR with specific primers. The RT-qPCR was performed in a reaction mixture of Hieff® qPCR SYBR Green Master Mix (Low Rox Plus) (YEASEN, Shanghai, China), template, primers, reverse transcriptase (YEASEN) and RNase-free water. Primer sequences are available upon request and their sequences were listed in Supplementary Table S1.

Reagents and antibodies

Lipopolysaccharide (LPS) (L9641) were purchased from Sigma-Aldrich (Missouri, United States). Methylcobalamin (HY-B0586), Z-DEVD-FMK (HY-12466) were purchased from MCE (New Jersey, United States). AGS-A (83207-58-3) were commercially purchased from Selleck (Houston, United States). Puromycin (abs9143) was purchased from Absin (Shanghai, China). RPMI-1640 and DMEM were obtained from Gibco. Nigericin (tlrl-nig) was obtained from InvivoGen (Toulouse, France). Antibody against Flag (M185-7) (1:2000) were purchased from MBL (Tokyo, Japan). Monoclonal rabbit anti-GSDME (Ab215191) (1:1000) and monoclonal rabbit anti-cleaved Caspase-3 (Ab32042) (1:1000) were purchased from Abcam (Cambridge, United Kingdom). Monoclonal rabbit anti-Caspase-3 (A2156) (1:1000) were purchased from Abclonal (Wuhan, China). Monoclonal rabbit anti-GSDMD (E9S1X) (1:1000), monoclonal rabbit anti-cleaved GSDMD (Asp276) (E3E3P) (1:1000), monoclonal rabbit anti-Caspase-1 (E2Z1C) (1:1000), monoclonal rabbit anti-cleaved Caspase-1 (Asp296) (E2G2I) (1:1000) were purchased from Cell Signaling Technology (Massachusetts, United States). Monoclonal anti-HRP-conjugated α-Tubulin (HRP-66031) (1:5000) was purchased from Proteintech (Wuhan, China). Human IL-1β ELISA Kit (DLB50) and Mouse IL-1β ELISA Kit (MLB00C) were purchased from R&D Systems (Minnesota, United States). LDH Cytotoxicity Assay Kit (C20300) was purchased from Invitrogen (California, United States).

Flow cytometry

Single-cell suspensions from the spleen were stained with different combinations of the following mAbs conjugated with FITC as our previously described (Wang C. et al., 2017). For cell surface maker staining, single-cell suspensions were incubated with the following Abs: FITC anti-CD3 (BioLegend, California, United States) in 0.2% BSA (BioSharp, Hefei, China) with PBS (pH 7.4) for 25 min at 4 °C. Cells were washed with PBS (400 g, 5 min, 4 °C) and fixed with 1% paraformaldehyde. Cells were determined using a FACS Calibur (BD Biosciences) system, and the data were analyzed using CellQuest Pro software (BD Biosciences, New Jersey, United States).

Methylcobalamin (MeCbl) treatment

MeCbl were commercially purchased from MCE. 5-day-old ICR mice were treated with MeCbl at the dose of 10 mg/kg within vehicle 24 h after challenge with EV-A71, followed by treatment once every two days for three times by intraperitoneal (i.p.) administration. The survival distribution for mice during the 14-d period is shown by curves.

Combination of MeCbl and AGS-A treatment

5-day-old WT BALB/c mice or BALB/c-nu−/− mice were treated with MeCbl via i.p. administration at a dose of 10 mg/kg 24 h after EV-A71 challenge, followed by treatment once every two days for three times, and administrated AGS-A via i.p. at a dose of 10 mg/kg 12 h after EV-A71 challenge, followed by treatment twice a day for 6 days as our previously described (Wang et al., 2025). The survival distribution for mice during the 14-d period is shown by curves.

Lentivirus-mediated gene stable expression and knockdown

The methods and materials of Lentivirus-mediated gene stable expression and knockdown were described in our previous study (Wang et al., 2022). Knockdown of GSDMD and GSDME was performed via lentiviral transduction in Jurkat cells. The targeting sequences of shRNAs for human GSDMD and GSDME were as follows: shGSDMD: 5′-GTGTGTCAACCTGTCTATCAA-3′; shGSDME: 5′- TGATGGAGTATCTGATCTT -3′. The pLKO.1 vector encoding non-specific shRNA as a negative control or a specific shRNA targeting one of the GSDMD components as noted above was transfected into 293T cells together with CG8.91 and PMD2.G. For stably expressing GSDME in Jurkat cells, GSDME was cloned into phage-3xFlag vector, named phage-GSDME-3xFlag, and then transfected into 293T cells with the packaging vectors pSPAX2 and pMD2G. Culture supernatants were harvested after transfection at 48 h.p.i. Jurkat cells were then infected with the supernatants containing lentiviral particles. After 48 h, cells were selected by 2 μg/mL puromycin for 2 days, and the knocking down effects were detected via Western blotting.

Western blot analysis

Cells treated as indicated were lysed with buffer (1% Triton X-100, 0.5% sodium deoxycholate, 0.1% SDS, 50 mM Tris, pH 7.5, 150 mM NaCl, 5 mM EDTA, and 10% glycerol). Cell supernatants were incubated with Trichloroacetic acid (TCA) overnight at 4 °C and centrifuged at 12,000 g for 10 min at 4 °C. The pellets were washed, mixed with SDS

loading buffer and boiled for 10 min for analysis. Cell lysates and supernatants were subjected to 10%–12% SDS-polyacrylamide gel electrophoresis (PAGE) and then transferred to polyvinylidene difluoride (PVDF) membranes (Millipore). Then, the membranes were blocked with 5% nonfat milk in TBST buffer (50 mM Tris/HCl, pH 7.4, 150 mM NaCl and 0.1% Tween-20) for 1–2 h, followed by incubation in primary antibody diluted in 5% nonfat milk-TBST for 12 h at 4 °C. Afterward, the membranes were incubated with the appropriate horseradish peroxidase (HRP)-conjugated secondary antibody diluted in 5% nonfat milk-TBST for 1 h. The expression of antigen was visualized using an enhanced chemiluminescence (ECL) kit (Millipore).

Cytotoxicity assay

Cell death was measured using culture supernatants by a lactate dehydrogenase (LDH) assay using CyQUANT™ LDH Cytotoxicity Assay Kit (Invitrogen) according to the manufacture's instructions. The cytotoxicity of MeCbl in Jurkat cells was measured by the CCK-8 assay using CCK-8 Kit (Invitrogen) according to the instructions.

Statistical analyses

All data were analyzed with GraphPad Prism (GraphPad Software, La Jolla, CA). Data are expressed as the mean SEM, and the significance of differences between groups was evaluated by using a parametric ANOVA test. A *P*-value of 0.05 was considered significant.

DATA AVAILABILITY

All data relevant to the study are included in the article or uploaded as supplementary information.

ETHICS STATEMENT

All animal research protocols strictly adhere to the 'Guidelines for the Care and Use of Laboratory Animals' at the Wuhan Institute of Virology, Chinese Academy of Sciences (CAS). All experiments comply with relevant regulatory standards. The experiments and protocols have been approved by the Ethics Committee of the Wuhan Institute of Virology (WIVA24202005).

AUTHOR CONTRIBUTIONS

Chong Wang: investigation, data curation, writing-original draft, funding acquisition; Bingyu Guo: methodology, validation; Yilin Li: validation, formal analysis; Xi Zhou: supervision, funding acquisition; Zongqiang Cui: supervision, writing-review & editing; Yujie Ren: conceptualization, supervision, writing-review & editing, funding acquisition.

CONFLICT OF INTEREST

Prof. Zongqiang Cui and Prof. Xi Zhou are editorial board members for *Virologica Sinica* and were not involved in the editorial review or the decision to publish this article. The authors declare no competing interest.

ACKNOWLEDGMENTS

This work was supported by the National Natural Science Foundation of China (22293033 to ZQ.C., 82522054 and 32100106 to YJ.R., 32200130 to C.W.), the Strategic Priority Research Program of CAS (XDC0200200 to YJ.R.), Hubei Province Natural Science Funds (2023AFA008 to X. Z.).

APPENDIX A. SUPPLEMENTARY DATA

Supplementary data to this article can be found online at https://doi.org/10.1016/j.virs.2026.05.006.

REFERENCES

Broz, P., Pelegrin, P., Shao, F., 2020. The gasdermins, a protein family executing cell death and inflammation. Nat. Rev. Immunol. 20, 143–157.
Carsetti, R., Quintarelli, C., Quinti, I., Mortari, E.P., Zumla, A., Ippolito, G., Locatelli, F., 2020. The immune system of children: the key to understanding SARS-CoV-2 susceptibility? Lancet. Child. Adolesc. 4, 414–416.
Chan, L.G., Parashar, U.D., Lye, M.S., Ong, F.G., Zaki, S.R., Alexander, J.P., Ho, K.K., Han, L.L., Pallansch, M.A., Suleiman, A.B., Jegathesan, M., Anderson, L.J., 2000. Deaths of children during an outbreak of hand, foot, and mouth disease in Sarawak, Malaysia: clinical and pathological characteristics of the disease. For the outbreak study group. Clin. Infect. Dis. 31, 678–683.
Chang, L.Y., Chang, I.S., Chen, W.J., Huang, Y.C., Chen, G.W., Shih, S.R., Juang, J.L., Shih, H.M., Hsiung, C.A., Lin, T.Y., Huang, L.M., 2008. HLA-A33 is associated with susceptibility to enterovirus 71 infection. Pediatrics 122, 1271–1276.
Chang, L.Y., Hsiung, C.A., Lu, C.Y., Lin, T.Y., Huang, F.Y., Lai, Y.H., Chiang, Y.P., Chiang, B.L., Lee, C.Y., Huang, L.M., 2006. Status of cellular rather than humoral immunity is correlated with clinical outcome of enterovirus 71. Pediatr. Res. 60, 466–471.
De Schutter, E., Roelandt, R., Riquet, F.B., Van Camp, G., Wullaert, A., Vandenabeele, P., 2021. Punching holes in cellular membranes: biology and evolution of gasdermins. Trends Cell Biol. 31, 500–513.
Fioravanti, C.H., 2012. Brazilian fitness programme registers health benefits. Lancet 380, 206.
He, W.T., Wan, H.Q., Hu, L.C., Chen, P.D., Wang, X., Huang, Z., Yang, Z.H., Zhong, C.Q., Han, J.H., 2015. Gasdermin D is an executor of pyroptosis and required for interleukin-1β secretion. Cell Res. 25, 1285–1298.
Ho, M., Chen, E.R., Hsu, K.H., Twu, S.J., Chen, K.T., Tsai, S.F., Wang, J.R., Shih, S.R., 1999. An epidemic of enterovirus 71 infection in Taiwan. Taiwan enterovirus epidemic working group. N. Engl. J. Med. 341, 929–935.
Huang, C.C., Liu, C.C., Chang, Y.C., Chen, C.Y., Wang, S.T., Yeh, T.F., 1999. Neurologic complications in children with enterovirus 71 infection. N. Engl. J. Med. 341, 936–942.
Lee, K.Y., 2016. Enterovirus 71 infection and neurological complications. Korean. J. Pediatr. 59, 395–401.
Liu, X., Zhang, Z., Ruan, J., Pan, Y., Magupalli, V.G., Wu, H., Lieberman, J., 2016. Inflammasome-activated gasdermin D causes pyroptosis by forming membrane pores. Nature 535, 153–158.
Lu, L., Su, S., Yang, H., Jiang, S., 2021. Antivirals with common targets against highly pathogenic viruses. Cell 184, 1604–1620.
Olin, A., Henckel, E., Chen, Y., Lakshmikanth, T., Pou, C., Mikes, J., Gustafsson, A., Bernhardsson, A.K., Zhang, C., Bohlin, K., 2018. Stereotypic immune system development in newborn children. Cell 174, 1277–1292.e14.
Rogers, C., Erkes, D.A., Nardone, A., Aplin, A.E., Fernandes-Alnemri, T., Alnemri, E.S., 2019. Gasdermin pores permeabilize mitochondria to augment caspase-3 activation during apoptosis and inflammasome activation. Nat. Commun. 10, 1689.
Shen, Y.X., Pan, Z.J., Zhang, L., Xue, W., Peng, M.L., Hu, P., Xu, H.M., Chen, M., 2019. Increased effector γδ T cells with enhanced cytokine production are associated with inflammatory abnormalities in severe hand, foot, and mouth disease. Int. Immunopharmacol. 73, 172–180.
Shi, J.J., Zhao, Y., Wang, K., Shi, X.Y., Wang, Y., Huang, H.W., Zhuang, Y.H., Cai, T., Wang, F.C., Shao, F., 2015. Cleavage of GSDMD by inflammatory caspases determines pyroptotic cell death. Nature 526, 660–665.
Simon, A.K., Hollander, G.A., McMichael, A., 2015. Evolution of the immune system in humans from infancy to old age. P. Roy. Soc. B-Biol. Sci. 282, 20143085.
Solomon, T., Lewthwaite, P., Perera, D., Cardoso, M.J., McMinn, P., Ooi, M.H., 2010. Virology, epidemiology, pathogenesis, and control of enterovirus 71. Lancet Infect. Dis. 10, 778–790.
Tan, X.J., Huang, X.Y., Zhu, S.L., Chen, H., Yu, Q.L., Wang, H.Y., Huo, X.X., Zhou, J.H., Wu, Y., Yan, D.M., Zhang, Y., Wang, D., Cui, A., An, H., Xu, W., 2011. The persistent circulation of enterovirus 71 in People's Republic of China: causing emerging nationwide epidemics since 2008. PLoS One 6, e25662.
Wang, C., Huang, M.H., Guo, B.Y., Zhou, X., Cui, Z.Q., Xu, Y., Ren, Y.J., 2025. Severe enterovirus A71 infection is associated with dysfunction of T cell immune response and alleviated by Astragaloside A. Virol. Sin. 40, 451–461.
Wang, C., Yang, R.Y., Yang, F.X., Han, Y., Ren, Y.J., Xiong, X.B., Wang, X.Y., Bi, Y.D., Li, L.J., Qiu, Y., Xu, Y., Zhou, X., 2022. Echovirus 11 infection induces pyroptotic cell death by facilitating NLRP3 inflammasome activation. PLoS Pathog. 18, e1010787.
Wang, C., Zhang, N., Qi, L.T., Yuan, J.L., Wang, K., Wang, K.L., Ma, S.C., Wang, H.L., Lou, W.J., Hu, P.D., Awais, M., Cao, S., Fu, Z.F., Cui, M., 2017. Myeloid-derived suppressor cells inhibit T follicular helper cell immune response in Japanese encephalitis virus infection. J. Immunol. 199, 3094–3105.
Wang, Y.P., Gao, W.Q., Shi, X.Y., Ding, J.J., Liu, W., He, H.B., Wang, K., Shao,, F., 2017. Chemotherapy drugs induce pyroptosis through caspase-3 cleavage of a gasdermin. Nature 547, 99–103.
Wei, R.C., Yang, C.F., Zeng, M., Terry, F., Zhu, K., Yang, C.H., Altmeyer, R., Martin, W., De Groot, A.S., Leng, Q.B., 2012. A dominant EV71-Specific CD4+T cell epitope is highly conserved among human enteroviruses. PLoS One 7, e51957.

Wu, X., Zhang, H., Qi, W., Zhang, Y., Li, J., Li, Z., Lin, Y., Bai, X., Liu, X., Chen, X., 2018. Nicotine promotes atherosclerosis via ROS-NLRP3-mediated endothelial cell pyroptosis. Cell. Death. Dis. 9, 171.

Xi, J.M., Ye, F., Wang, G.Z., Han, W., Wei, Z.Z., Yin, B., Yuan, J.G., Qiang, B.Q., Peng, X.Z., 2019. Polypyrimidine tract-binding protein regulates enterovirus 71 translation through interaction with the internal ribosomal entry site. Virol. Sin. 34, 66–77.

Xu, W.F., Wang, Y., Cui, S., Zheng, Q.L., Lin, Y.H., Cui, Q.Q., Xie, Y.X., Zeng, Y.M., Zhang, C., Li, Y.J., 2025. Methylcobalamin protects against liver failure via engaging gasdermin E. Nat. Commun. 16, 1233.

Xu, Y.J., Zheng, L., Hu, Y.W., Wang, Q., 2018. Pyroptosis and its relationship to atherosclerosis. Clin. Chim. Acta 476, 28–37.

Yang, K.D., Yang, M.Y., Li, C.C., Lin, S.F., Chong, M.C., Wang, C.L., Chen, R.F., Lin, T.Y., 2001. Altered cellular but not humoral reactions in children with complicated enterovirus 71 infections in Taiwan. J. Infect. Dis. 183, 850–856.

Zhang, Z.W., Zhang, H., Li, D.B., Zhou, X.P., Qin, Q., Zhang, Q.Y., 2021. Caspase-3-mediated GSDME induced Pyroptosis in breast cancer cells through the ROS/JNK signalling pathway. J. Cell Mol. Med. 25, 8159–8168.

Zhao, M.Q., Wang, L.H., Lian, G.W., Lin, Z.F., Li, Y.H., Guo, M., Chen, Y., Liu, X.M., Zhu, B., 2020. Characterization of lymphocyte subsets in peripheral blood cells of children with EV71 infection. J. Microbiol. Immunol 53, 705–714.